Pedometer-free Geomagnetic Fingerprinting with Casual Walking Speed

HANG WU, JIAJIE TAN, and S.-H. GARY CHAN, The Hong Kong University of Science and Technology, China

The geomagnetic field has been wildly advocated as an effective signal for fingerprint-based indoor localization due to its omnipresence and local distinctive features. Prior survey-based approaches to collect magnetic fingerprints often required surveyors to walk at constant speeds or rely on a meticulously calibrated pedometer (step counter) or manual training. This is inconvenient, error-prone, and not highly deployable in practice. To overcome that, we propose Maficon, a novel and efficient pedometer-free approach for geo**ma**gnetic **fi**ngerprint database **con**struction. In Maficon, a surveyor simply walks at *casual* (arbitrary) speed along the survey path to collect geomagnetic signals. By correlating the features of geomagnetic signals and accelerometer readings (user motions), Maficon adopts a self-learning approach and formulates a quadratic programming to accurately estimate the walking speed in each signal segment and label these segments with their physical locations. To the best of our knowledge, Maficon is the first piece of work on pedometer-free magnetic fingerprinting with casual walking speed. Extensive experiments show that Maficon significantly reduces walking speed estimation error (by more than 20%) and hence fingerprint error (by 35% in general) as compared with traditional and state-of-the-art schemes.

CCS Concepts: • **Networks** → **Location based services**; • **Human-centered computing**;

Additional Key Words and Phrases: Geomagnetic field, site survey, fingerprint database construction, sequence matching, machine learning, speed estimation

ACM Reference format:
Hang Wu, Jiajie Tan, and S.-H. Gary Chan. 2021. Pedometer-free Geomagnetic Fingerprinting with Casual Walking Speed. *ACM Trans. Sen. Netw.* 18, 1, Article 8 (September 2021), 21 pages.
https://doi.org/10.1145/3470850

1 INTRODUCTION

The geomagnetic field has been widely studied for indoor localization [7, 14, 17, 23, 33]. This is mainly due to its omnipresence and its local distortion caused by ferromagnetic materials (such as pillars and gates), serving as a good location differentiator. Without the need for infrastructure installation, it greatly eases the deployment effort. Furthermore, a user can sample geomagnetic fields with a **commercial off-the-shelf (COTS)** smartphone at high frequency (typically in the

This work was supported, in part, by the Hong Kong General Research Fund under grant number 16200120.
Authors' address: H. Wu, J. Tan (corresponding author), and S.-H. Gary Chan, Department of Computer Science and Engineering, The Hong Kong University of Science and Technology, Clear Water Bay, Kowloon, Hong Kong, People's Republic of China; emails: hwuav@connect.ust.hk, {jtanad, gchan}@cse.ust.hk.

1550-4859/2021/09-ART8 $15.00
https://doi.org/10.1145/3470850

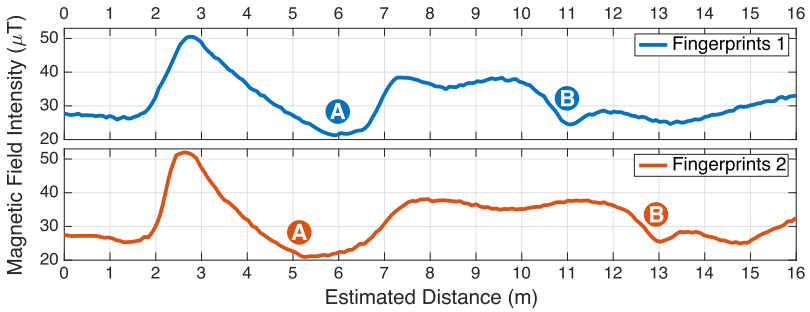

Fig. 1. Geomagnetic fingerprints collected from two casual walks on the same path. The walks do not follow constant walking speed, while the locations (i.e., estimated distance to the starting point) are computed by assuming so. The character labels indicate the magnetic snippets of the same physical locations of the two walks, which clearly shows significant labeling errors.

order of 50 samples per second) while walking. This fast sampling leads to fine-grained location estimation and hence continuous navigation.

Fingerprinting approaches are often used for geomagnetic localization, where the geomagnetic *fingerprints*, defined as the field values labeled with their locations, are collected through a process called *site survey*. In the process, a surveyor first defines paths in the covered area of the floor map [22, 33]. Holding a magnetic sensing device (such as a smartphone), he or she then walks along the planned paths while collecting geomagnetic samples and their timestamps. To mitigate measurement noise, such walks are often repeated several times.

Assessing accurately walking speed is key to correctly *label* the geomagnetic samples with their corresponding locations (hence forming fingerprints). Many approaches require the surveyor to walk strictly at a constant speed along the planned paths (see, e.g., [7, 30] and [33]). This is hardly practical or convenient in reality, and may lead to severe labeling, and hence localization, error. Figure 1 illustrates an example of geomagnetic fingerprints generated from two casual walks that violate the constant speed requirement. Despite similar field patterns, the two paths display significant inconsistency in field labeling. For instance, the labeling discrepancy for snippets "A" and "B" are about 1 m and 2 m, respectively. This can lead to substantial labeling errors due to the wrong location labels.

To overcome the constant speed requirement, the pedometer (or step counter) has been recently studied to estimate survey speeds [6, 22]. Using a step model that returns the stride length of the pedestrian, the pedometer can then estimate the walking distance based on which the geomagnetic samples are labeled. The performance of such an approach, however, depends strongly on model selection and training. To accommodate user heterogeneity, meticulous user training and device calibration are needed to set these parameters. This is time-consuming, error-prone, inconvenient, and inefficient in practice. It also makes strong behavior assumptions on users walking and holding the survey device, which is often not realistic.

We propose **Maficon**, a novel, efficient, and pedometer-free *site survey* approach using self-learning for geo**ma**gnetic **fi**ngerprint database **con**struction. Maficon estimates surveyors' walking speed to accurately label the signals (i.e., fingerprinting). It reduces the site survey to a *casual* process of arbitrary walking speed. Without a pedometer, it does not make any assumption on user behavior and does not need any step model for training or calibration. Using the embedded sensors of a phone, a surveyor follows the pre-defined path several times by simply walking at random and casual speed, with the phone timestamping the geomagnetic field and acceleration readings along the way. Given these walk sequences with their collected data, Maficon estimates

(a) Inter-sequence segments. (b) Intra-sequence segments.

Fig. 2. An illustration of inter- and intra-sequence segments. Each row represents a sequence (readings over time) sliced with segments. The dotted lines indicate the same physical positions in different sequences. *SEG*1 and *SEG*2 in (a) are aligned inter-sequence segments. *SEG*2 and *SEG*3 in (b) are intra-sequence segments.

the speed in each segment of the path by considering the correlation of the magnetic field in the segments and relating it with the acceleration measurements. The fingerprinting process of Maficon is highly accurate, easy to execute, and universally deployable in real-world scenarios. To the best of our knowledge, this is the first piece of work that studies the site survey process of magnetic fields under casual walking speed.

The major contributions of this work are summarized as follows:

- *Quadratic programming for survey speed estimation through different types of speed ratios:* Direct estimation of surveyors' walking speeds usually relies on complex mobility models and tedious training or calibration for heterogeneous users/devices. To overcome this, we formulate the survey speed estimation problem as a **quadratic programming (QP)** by fusing the *speed ratio*s of *inter-* and *intra-*sequence path segments. Referring to Figure 2, *inter-sequence* segments represent the segments over the same physical space in different walk sequences.[1] These speed ratios reflect the relative speeds between different walks (inter-sequence) and speed variation of individual walks (intra-sequence). They can be obtained through multimodal signals (magnetic fields and accelerations) and essentially reduce the heterogeneity factors in measurements. Such QP can be solved efficiently in Maficon to obtain accurate survey speeds.
- *Personalized speed ratio estimation without any prior training:* We propose to employ novel sequence alignment and self-learning techniques to estimate different types of speed ratios without any prior training effort. By applying modified **multiple sequence alignment (MSA)**, we efficiently estimate inter-sequence speed ratios based on the correspondence of magnetic fields. For intra-sequence segments, we use a regression model to correlate acceleration patterns with speed ratios. In contrast to other schemes that require huge efforts to gather training datasets [19], we propose a novel self-learning mechanism that generates labeled datasets based on inter-sequence segments and their estimated speed ratios. Maficon hence requires neither prior training nor manual data labeling. Furthermore, since the model is learned only from the current surveyor, Maficon is personalized and naturally adapts to heterogeneous devices or users.
- *Extensive experiments results:* We have implemented Maficon in smartphones and conducted extensive experiments in different typical types of areas (including corridor, open area, and mixed region) to validate its simplicity, implementability, accuracy, and deployability. Our results show that Maficon improves the accuracy of walking speed estimation and geomagnetic fingerprint database significantly as compared with other traditional or state-of-the-art schemes (cutting speed error by more than 20% and fingerprint error by 35% in general), without the requirements of pedometer and constant walking speed.

[1]Unless otherwise specified, we refer to inter-sequence segments as aligned segments in different sequences.

Table 1. Major Symbols Used in Maficon

Symbol	Definition
SEQ_i	Sequence bundle of the ith walk
$SEG_{i,k}$	The kth segment in SEQ_i
$\boldsymbol{B}_{i,k}$	Geomagnetic sequence collected in $SEG_{i,k}$
$\boldsymbol{A}_{i,k}$	Acceleration sequence collected in $SEG_{i,k}$
$\boldsymbol{b}$	Orientation-invariant feature vector of a magnetic sample
M	Number of walks (sequences) along a survey path
L	Number of segments of a sequence
W	Number of geomagnetic samples in a segment
$N_{i,k}$	Number of geomagnetic samples in $SEG_{i,k}$
$v_{i,k}$	Average walking speed in $SEG_{i,k}$
$\tau_{i,k}$	Time duration of $SEG_{i,k}$
$m_{i,j}(k)$	Inter-sequence speed ratio of $v_{i,k}$ to $v_{j,k}$
$r_i(k,l)$	Intra-sequence speed ratio of $v_{i,k}$ to $v_{i,l}$
s	Physical length of a survey path

The remainder of the article is organized as follows. We first introduce the preliminaries and system framework in Section 2. Then, we discuss how to compute inter-sequence speed ratios between aligned magnetic segments in Section 3. In Section 4, we present our learning-based approach to obtain speed ratios between pairwise intra-sequence segments. Section 5 presents the problem formulation to calculate the absolute walking speed in each segment and how to label the magnetic signals with their locations. The illustrative experimental results are presented in Section 6. We introduce related works of Maficon in Section 7. Finally, we discuss some deployment and application topics in Section 8 and conclude in Section 9.

2 PRELIMINARIES AND SYSTEM FRAMEWORK

In this section, we present the preliminaries and system framework of Maficon. Section 2.1 introduces the preliminaries and problem formulation. In Section 2.2, we illustrate the system framework of Maficon. The major symbols used in this article are summarized in Table 1.

2.1 Preliminaries and Problem Formulation

When a surveyor walks along a pre-defined path, both magnetic field and acceleration readings are recorded by his or her carried smartphone. Note that raw measurements are under the coordinate system of the smartphone itself, which cannot be compared directly if the attitudes of devices are different. To address it, we transform the original magnetic measurement sample $\tilde{\boldsymbol{b}} = \langle b_x, b_y, b_z \rangle$ into an orientation-invariant feature vector $\boldsymbol{b} = \langle b_s, b_v, b_h \rangle$ [16, 22, 30], where b_x, b_y, and b_z are raw magnetic measurements the under phone's coordinate system; b_s is the magnitude of $\tilde{\boldsymbol{b}}$, i.e.,

$$b_s = \|\tilde{\boldsymbol{b}}\|_2 = \sqrt{b_x^2 + b_y^2 + b_z^2}; \tag{1}$$

and b_v and b_h are the vertical and horizontal components of $\tilde{\boldsymbol{b}}$ with respect to gravity, respectively. In particular,

$$b_v = b_y \sin\phi - b_x \cos\phi \sin\theta + b_z \cos\phi \cos\theta, \tag{2}$$

$$b_h = \left[(b_x \cos\theta + b_z \sin\theta)^2 + \left(b_y \cos\phi + b_x \sin\phi \sin\theta - b_z \sin\phi \cos\theta \right)^2 \right]^{\frac{1}{2}}, \tag{3}$$

where the attitude of the device, in terms of roll ϕ, pitch θ, and yaw ψ, can be obtained from the rotation matrix provided by the device [36]. On the other hand, we take the magnitude of acceleration to represent the overall motion, i.e., $a = \|\tilde{\boldsymbol{a}}\|_2$, with $\tilde{\boldsymbol{a}}$ being the raw acceleration measurement under the phone's coordinate system.

In a typical survey process, the surveyor walks a survey path for M times at his or her own (casual or leisure) speeds. Given the homogeneous sampling frequency ω (i.e., ω samples are obtained per second), sensor measurements during the ith walk can be represented as a multimodal *sequence*, i.e., $SEQ_i = \langle \boldsymbol{B}_i, \boldsymbol{A}_i \rangle$, where $\boldsymbol{B}_i = \{\boldsymbol{b}_{i,n} \mid 1 \le n \le N_i\}$ is the magnetic field sequence and $\boldsymbol{A}_i = \{a_{i,n} \mid 1 \le n \le N_i\}$ is the acceleration sequence, and N_i denotes the number of collected samples. For a survey path, we can obtain a set of sequences $\mathcal{P} = \{SEQ_i \mid 1 \le i \le M\}$.

The objective of Maficon is to infer the location $\boldsymbol{l}_{n_*}$ of the collected magnetic signal at time t_{n_*} of each sequence. Because the survey path is known in advance, we can directly obtain $\boldsymbol{l}_{n_*}$ based on the walking distance d_{n_*} to the starting point. Further note that d_{n_*} can be estimated by

$$d_{n_*} = \sum_{n=1}^{n_*} \tilde{v}_n (t_n - t_{n-1}) = \sum_{n=1}^{n_*} \frac{\tilde{v}_n}{\omega}, \tag{4}$$

where $\tilde{v}_n$ is the speed between the consecutive timestamps t_{n-1} and t_n. We can hence reduce the fingerprinting problem to estimating walking speed in survey paths.

Since the walking speeds of surveyors do not change frequently, we partition each sequence into L segments and consider its average speed to be the survey speed in the segment (the segmentation strategy will be discussed in Section 3.3). We use $SEG_{i,k}$ to denote the kth segment in the ith sequence SEQ_i, and hence $SEQ_i = \{SEQ_{i,k} \mid 1 \le k \le L\}$, where $SEQ_{i,k} = \langle \boldsymbol{B}_{i,k}, \boldsymbol{A}_{i,k} \rangle$, with $\boldsymbol{B}_{i,k}$ being the subsequence of magnetic fields and $\boldsymbol{A}_{i,k}$ being the subsequence of accelerations. The speed in a segment $SEG_{i,k}$ is denoted by $v_{i,k}$.

Given the above, the *survey speed estimation* problem can be stated as: given a set of sequences $\{SEQ_i \mid 1 \le i \le M\}$ along a survey path of length s, where each sequence can be segmented as $SEQ_i = \{SEQ_{i,k} \mid 1 \le k \le L\}$, we aim to estimate the walking speed of each segment $v_{i,k}$ $(1 \le i \le M, 1 \le k \le L)$.

Maficon jointly considers the speed ratios of inter- and intra-sequence segments to estimate walking speed in segments. Note that we consider that the inter-sequence segments are *aligned*; i.e., they are collected in the same region of the survey path. For two aligned segments $SEG_{i,k}$ and $SEG_{j,k}$ in the ith and jth sequences, the inter-sequence speed ratio is defined as

$$m_{i,j}(k) \triangleq \frac{v_{i,k}}{v_{j,k}}. \tag{5}$$

Similarly, we define the intra-sequence speed ratio of two segments $SEG_{i,k}$ and $SEG_{i,l}$ in the same sequence as

$$r_i(k,l) \triangleq \frac{v_{i,k}}{v_{i,l}}. \tag{6}$$

2.2 System Framework

We show in Figure 3 the system framework of Maficon. Given a set of signal sequences collected from the same survey path, Maficon fingerprints geomagnetic fields using the speed ratios between inter-sequence or intra-sequence segment pairs. It consists of the following three major steps:

(1) *Inter-sequence speed ratio estimation*: Maficon first estimates the inter-sequence speed ratio by identifying the location correspondence among multiple sequences according to their magnetic sequence alignments. Different from traditional approaches of **dynamic time**

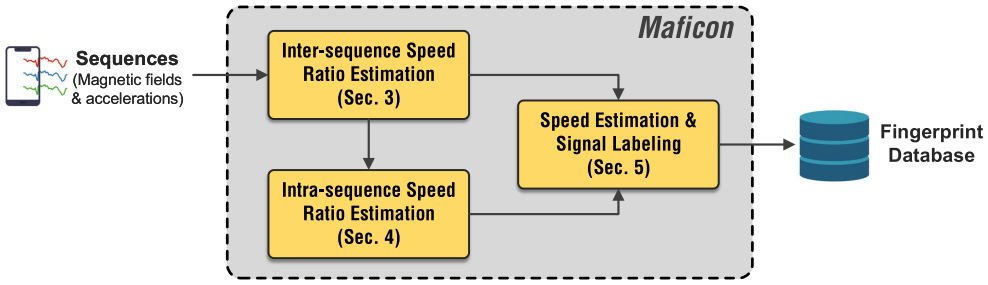

Fig. 3. The system framework of Maficon.

warping (DTW) that align only two sequences, Maficon employs a novel and efficient hierarchical method based on DTW to accurately align all the sequences of the same path simultaneously. By comparing the duration of the aligned segment pairs, the speed ratios between them can then be easily obtained.

(2) *Intra-sequence speed ratio estimation*: Maficon next estimates the speed ratios between intra-sequence segments. To achieve this, it learns, by employing **support vector regression (SVR)**, the correlation between the features of acceleration readings in both time and frequency domains (e.g., variance, frequency, energy, etc.) and the speed ratios of pairwise aligned segments given in Step (1) above. After such training, Maficon generates the speed ratios between all the pairs of intra-sequence segments using the model.

(3) *Speed estimation and signal labeling*: With both inter- and intra-sequence speed ratios as obtained in Steps (1) and (2), Maficon finally derives the absolute walking speed in each segment by formulating the problem as a QP. According to the estimated walking speeds, it then labels the collected signal samples with their precise locations.

3 INTER-SEQUENCE SPEED RATIO ESTIMATION

In this section, we identify the inter-sequence segments from magnetic sequences and estimate their speed ratios. We first discuss how to align two magnetic sequences in Section 3.1. Then, we propose an alignment algorithm for multiple sequences in Section 3.2. Finally, we discuss the segmentation strategy and obtain the inter-sequence speed ratios based on the alignment results in Section 3.3.

3.1 Sequence Alignment for Two Sequences

When surveyors walk through the same area several times, similar patterns of magnetic fields can be measured. However, samples in one sequence usually do not have a one-to-one correspondence to the samples in another due to their dynamic and inconsistent traveling speeds. Figure 4 demonstrates such an example. We can observe that, due to the varied walking speeds, those sequences (colored curves) have similar trends but are locally scaled in time. This inspires us to learn the speed relation between two segments from their magnetic sample matching, which is also known as *alignment*.

DTW [3] is an effective algorithm that uses dynamic programming to find an optimal alignment among two sequences. The algorithm has been wildly applied in sequence analysis and shape matching [35]. In Maficon, we adopt a modified DTW to align two magnetic sequences.

Note that constant offsets of magnetic measurements are often observed due to heterogeneous devices and/or sensor bias [22]. To mitigate such influence, Maficon employs a mean-removal method when comparing two magnetic vectors. That is, we define the distance function between

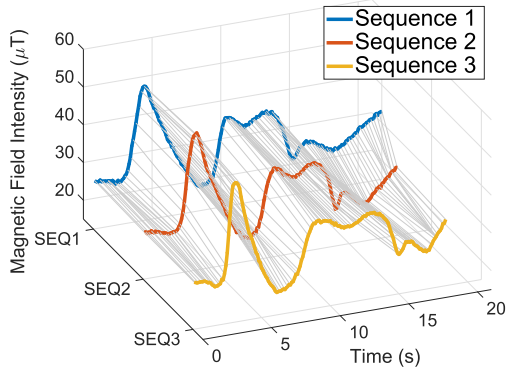

Fig. 4. An example of multiple magnetic sequences collected from the same survey path and the corresponding sequence alignment.

two magnetic field feature vectors, say, the mth sample in the ith sequence $\boldsymbol{b}_{i,m}$ and the nth sample in the jth sequence $\boldsymbol{b}_{j,n}$, as

$$\delta(\boldsymbol{b}_{i,m}, \boldsymbol{b}_{j,n}) = C \cdot \sum_{\gamma=-\Gamma}^{\Gamma} \left\| (\boldsymbol{b}_{i,m+\gamma} - \boldsymbol{\mu}_{i,m}) - (\boldsymbol{b}_{j,n+\gamma} - \boldsymbol{\mu}_{j,n}) \right\|_2 , \tag{7}$$

where $\boldsymbol{\mu}_{i,m} = C \cdot \sum_{\gamma=-\Gamma}^{\Gamma} \boldsymbol{b}_{i,m+\gamma}$ with $C = 1/(2\Gamma+1)$ and Γ is the parameter of window length. In this article, we set $\Gamma = 5$ empirically. With the distance function above, we can perform the adapted DTW to construct the optimal alignment between two magnetic sequences.

3.2 Sequence Alignment for Multiple Sequences

Note that the above approach only works for pairwise sequence alignment because the matching does not guarantee the consistency among multiple sequences. In practice, however, the number of collected sequences M is usually greater than two in order to mitigate measurement noise. Indeed, the **multiple sequence alignment (MSA)** problem itself has been proved to be an NP-complete problem [29], and the time complexity of the naïve method for all sequence combinations is $O(N^M)$, where N is the length of the longest sequence. To reduce computational complexity while maintaining alignment accuracy, Maficon employs a hierarchical progressive alignment method [15].

The progressive alignment iteratively conducts pairwise aligning from the most similar pair to the most dissimilar one. We illustrate the major procedures of MSA in Algorithm 1. At each iteration, we first find the pair of magnetic sequences with minimum DTW distance, say $\boldsymbol{B}_i$ and $\boldsymbol{B}_j$ (Line 3). Let the alignment between $\boldsymbol{B}_i$ and $\boldsymbol{B}_j$ be $\Gamma_{i,j} = \{(\boldsymbol{b}_{i,f(\eta)}, \boldsymbol{b}_{j,g(\eta)})\}$, where $\boldsymbol{b}_{i,f(\eta)}$ and $\boldsymbol{b}_{j,g(\eta)}$ are the ηth pair of matched samples in $\boldsymbol{B}_i$ and $\boldsymbol{B}_j$, respectively; the index $1 \le \eta \le \max(N_i, N_j)$, where N_i and N_j are the numbers of samples of the two sequences, respectively. The two sequences $\boldsymbol{B}_i$ and $\boldsymbol{B}_j$ are then replaced with $\boldsymbol{B}' = \{\boldsymbol{b}'_\eta \mid 1 \le \eta \le \max(N_i, N_j)\}$, where $\boldsymbol{b}'_\eta = (\boldsymbol{b}_{i,f(\eta)} + \boldsymbol{b}_{j,g(\eta)})/2$ (this operation is named as `Merge` in Line 6). The above procedure repeats until only one sequence $SEQ^\star$ remains. The overall alignment among all the sequences can be obtained by tracing the previous alignments. Note that each magnetic sample corresponds to a specific physical location. We can interpret that the alignment not only associates all the magnetic samples from multiple sequences but also identifies the same physical location among different walks. The complexity of MSA is $O(M^3N^2)$, where N is the number of samples in the longest sequence, which is efficient in practice.

ALGORITHM 1: Multiple Magnetic Sequence Alignment

input : A set of magnetic sequences $\mathcal{B} = \{\boldsymbol{B}_1, \boldsymbol{B}_2, ...\}$
output: The overall alignment $\boldsymbol{\Gamma}$ among $\mathcal{B}$

$\boldsymbol{\Gamma} \leftarrow \emptyset$;
while $|\mathcal{B}| > 1$ **do**
  $i, j \leftarrow \arg\min_{\phi,\psi}$ DTW_distance$(\boldsymbol{B}_\phi, \boldsymbol{B}_\psi)$;
  $\Gamma_{i,j} \leftarrow$ DTW$(\boldsymbol{B}_i, \boldsymbol{B}_j)$;
  $\boldsymbol{\Gamma} \leftarrow \boldsymbol{\Gamma} \cup \Gamma_{i,j}$;
  $\boldsymbol{B}' \leftarrow$ Merge$(\boldsymbol{B}_i, \boldsymbol{B}_j)$;
  Replace $\boldsymbol{B}_i$ and $\boldsymbol{B}_j$ with $\boldsymbol{B}'$ in $\mathcal{B}$;
end
return $\boldsymbol{\Gamma}$;

3.3 Sequence Segmentation and Inter-sequence Speed Ratio Estimation

Given the alignments among all the sequences, we can slice them into multiple aligned segments. To be specific, we first slice the ultimate sequence $SEQ^\star$ with length $N^\star$ into L non-overlapping segments with length W, where $L = \lceil N^\star / W \rceil$. Following the obtained alignments, other sequences can also be segmented based on the slicing points in $SEQ^\star$. As a result, all the sequences are sliced into L segments, and those aligned segments in different walks correspond to the same physical distance (thus the same walking distance).

The inter-sequence speed ratio of aligned segments can be computed according to the traveling time in segments. Let ω be the sampling frequency of the survey device. For the kth aligned segments $SEG_{i,k}$ and $SEG_{j,k}$ $(1 \le k \le L)$, we denote the number of magnetic samples in the corresponding segment as $N_{i,k}$ and $N_{j,k}$, respectively. We further denote the average walking speed within $SEG_{i,k}$ and $SEG_{j,k}$ as $v_{i,k}$ and $v_{j,k}$, respectively. The above distance relationship can be expressed as

$$v_{i,k} \cdot \frac{N_{i,k}}{\omega} = v_{j,k} \cdot \frac{N_{j,k}}{\omega}. \tag{8}$$

Or equivalently, the inter-sequence speed ratio $m_{i,j}(k)$ between two aligned segments $SEG_{i,k}$ and $SEG_{j,k}$ can be calculated by

$$m_{i,j}(k) = \frac{v_{i,k}}{v_{j,k}} = \frac{N_{j,k}}{N_{i,k}}. \tag{9}$$

4 INTRA-SEQUENCE SPEED RATIO ESTIMATION

In this section, we present a novel machine learning approach to compute the intra-sequence speed ratios without prior training. We discuss features extracted from accelerations in Section 4.1, followed by the design of the self-generating training dataset based on inter-sequence segments in Section 4.2. In Section 4.3, we discuss model selection and prediction of intra-sequence speed ratios.

4.1 Feature Extraction

Intuitively, accelerometers on smartphones are capable of capturing detailed information of user motions, and hence the dynamics of walking speed can also be reflected in sensor reading variations. Therefore, we employ a regression model between motion features and speed ratios so that the intra-sequence speed ratios can be obtained from their acceleration readings.

For each segment, we extract features from its acceleration measurements in both time and frequency domains. To avoid the influence of device orientation, we use only the magnitude of

Table 2. Features Extracted from Acceleration Segments

Feature	Category	Calculation
Mean	Time domain	$\mu = \frac{1}{N}\sum_{n=1}^{N} a_n$
Variance	Time domain	$\sigma^2 = \frac{1}{N}\sum_{n=1}^{N} (a_n - \mu)^2$
Standard deviation	Time domain	$\sigma = \sqrt{\frac{1}{N}\sum_{n=1}^{N} (a_n - \mu)^2}$
Mean energy	Time domain	$E = \frac{1}{N}\sum_{n=1}^{N} a_n^2$
Spectral shape mean	Frequency domain	$\mu_s = \frac{1}{C}\sum_{\eta=1}^{H} \eta\, S(\eta)$
Spectral shape standard deviation	Frequency domain	$\sigma_s = \sqrt{\frac{1}{C}\sum_{\eta=1}^{H} (\eta - \mu_s)^2\, S(\eta)}$
Spectral shape skewness	Frequency domain	$\gamma_s = \frac{1}{C}\sum_{\eta=1}^{H} ((\eta - \mu_s)/\sigma_s)^3\, S(\eta)$
Spectral shape kurtosis	Frequency domain	$\kappa_s = \frac{1}{C}\sum_{\eta=1}^{H} ((\eta - \mu_s)/\sigma_s)^4\, S(\eta) - 3$

accelerations. Let $\boldsymbol{A}$ denote the sequence of acceleration magnitudes of a segment with length H. In the frequency domain, we apply **discrete Fourier transform (DFT)** to convert $\boldsymbol{A}$ into spectrum S. We use $S(\eta)$ to denote the ηth frequency component in the spectrum S, and $C = \sum_{\eta=1}^{H} S(\eta)$. We extract features in each domain to capture the user mobilities, such as mean, variance, standard deviation, energy, and so forth. Table 2 lists the selected features.

Note that the above features are extracted from a single segment, which may not well-characterize the motion dynamics between segments. We hence leverage arithmetic operations, i.e., subtraction and division, to reflect their difference. Formally, let x_α and x_β be the same feature extracted from two segments $\boldsymbol{A}_\alpha$ and $\boldsymbol{A}_\beta$, respectively. We take $x_\alpha - x_\beta$ and x_α / x_β as the new features. Thereby, we are able to obtain the feature vector $\Delta \boldsymbol{x}_{\alpha,\beta}$ with $8 \times 2 = 16$ dimensions. In addition, we adopt min-max scaling to normalize each feature into $[0, 1]$.

We conduct experiments to investigate the effectiveness of the extracted features. The acceleration sequences of four users are collected when they walk in a corridor. Their walking speed (hence speed ratios) are manually labeled according to the captured simultaneous video (see Section 6.1 for detailed description). Figure 5 illustrates the results of univariate statistical tests including F-test and mutual information [9]. F-test usually depicts the linearity between features and labels, while mutual information reflects the general dependency. In F-test statistics, we can see that the difference of shape features in the frequency domain demonstrates a strong linear relationship with the speed ratio. The quotients among shape features achieve high mutual information. Considering that both types of features contain certain domain knowledge, we include them in the selected features to enhance the generality and robustness of the system.

4.2 Self-generation of Training Dataset

Traditional learning-based approaches require a large training dataset of acceleration and speed to train the model [19]. Since such a dataset is usually collected offline and labeled manually, it brings extra burdens and restricts model generality against heterogeneous users or devices. To address this, Maficon extracts inter-sequence segments and uses the magnetic alignment method discussed in Section 3 to automatically label segment pairs. Thus, the training dataset can be "self-generated."

The segmentation strategy discussed in Section 3.3 produces only non-overlapping segments, causing the dataset to be not sufficient for model training. To increase the number of training samples, a sliding window is applied. Recall that we have already obtained the multiple sequence alignment and the ultimate sequence $SEQ^\star$ in Section 3. We extract $seg_u^\star$ $(1 \le u \le Q)$ from $SEQ^\star$ by using a sliding window of size W with 25% overlap between subsequent windows, where the

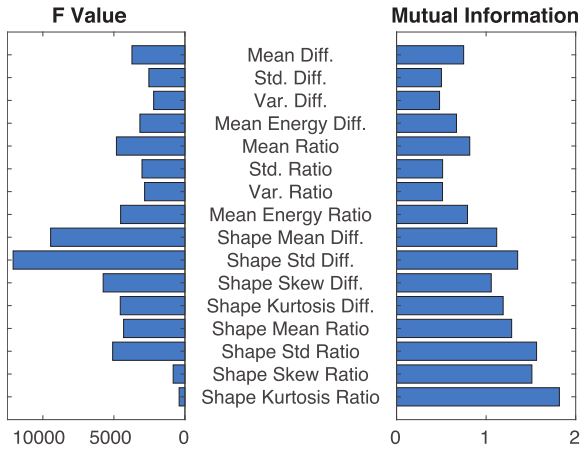

Fig. 5. Univariate statistical tests (F-test and mutual information) of features.

number of segments $Q = \max(1, \lceil 4N^\star/W \rceil - 3)$. For each $seg_u^\star$, we can thus find the matched segment $seg_{i,u}$ in SEQ_i according to the multi-sequence alignment result. Note that we use a different notion *seg* here to describe the segments obtained by the sliding window strategy as opposed to the non-overlapped segments *SEG* in Section 3.3, and segments *seg* are only used for training dataset generation. Thus, we can obtain the training set containing feature vectors $\{\Delta \boldsymbol{x}_{(i,u),(j,u)}\}$ and corresponding speed ratio labels $\{m_{i,j}(u)\}$, where $1 \le i, j \le M,\ i \ne j, 1 \le u \le Q$.

An important feasibility criterion of the above generation process is that both inter- and intra-sequence features lay on the same distribution. To validate this, we conduct experimental studies by visualizing the feature distributions of both inter- and intra-sequence segments in the previous dataset (Section 4.1). Note that, as the features are located in high dimensional space, we further perform **principal component analysis (PCA)** to project data to the 2-D space. Figure 6(a) compares the feature distributions in both categories, and Figures 6(b) and 6(c) demonstrate the distributions with speed ratio labels, respectively. We can clearly observe that both features and their corresponding labels are distributed similarly in the two cases. This validates that the intrinsic relationships between user motions and speed ratios are analogous.

4.3 Regression Model and Prediction

We finally discuss model selection and speed ratio prediction. Maficon is compatible with various regression models, such as linear regression, SVR, **artificial neural network (ANN)**, **k-nearest neighbors regression (k-NN)**, and so forth. We adopt SVR [4] in our implementation because it not only captures non-linear relationships well but also is efficient to train. Further performance comparison among different regression models can be found in Section 6.

We use the trained model to predict the intra-sequence speed ratio, i.e., $r_i(k,l) = v_{i,k}/v_{i,l}$, given the feature vector $\Delta \boldsymbol{x}_{(i,k),(i,l)}$ extracted from the acceleration sequences $\boldsymbol{A}_{i,k}$ and $\boldsymbol{A}_{i,l}$ of intra-sequence segments $SEG_{i,k}$ and $SEG_{i,l}$, respectively ($1 \le i \le M$, $1 \le k, l \le L$, $k \ne l$). Note that in the whole process, Maficon does not require any manual labeling or initial velocity, which is much more efficient than other works [6, 19].

5 SPEED ESTIMATION AND SIGNAL LABELING

In this section, we present how Maficon estimates accurate walking speeds based on inter- and intra-sequence speed ratios jointly and discuss labeling collected magnetic signals with corresponding locations.

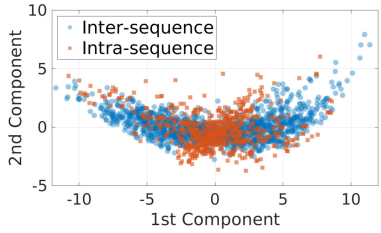

(a) Distribution comparison

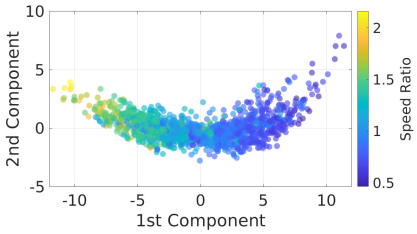

(b) Inter-sequence

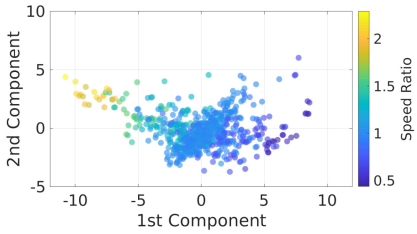

(c) Intra-sequence

Fig. 6. Visualization of the distributions of acceleration features using PCA.

Since walking speeds should fit both inter-sequence and intra-sequence ratios among segments, we formulate the walking speed estimation problem as the following QP optimization problem:

$$\begin{aligned} \underset{\boldsymbol{v}}{\text{minimize:}} \quad & \sum_{i=1}^{M} \sum_{\substack{j=1 \\ j \neq i}}^{M} \sum_{k=1}^{L} \| v_{i,k} - m_{i,j}(k) \cdot v_{j,k} \|^2 \\ & + \sum_{i=1}^{M} \sum_{k=1}^{L} \sum_{\substack{l=1 \\ l \neq k}}^{L} \| v_{i,k} - r_i(k,l) \cdot v_{i,l} \|^2, \end{aligned} \tag{10}$$

$$\text{subject to:} \quad \sum_{k=1}^{L} v_{i,k} \cdot \tau_{i,k} = s, \quad \forall 1 \leq i \leq M, \tag{11}$$

$$v_{i,k} > 0, \quad \forall 1 \leq i \leq M, \forall 1 \leq k \leq L, \tag{12}$$

where $\tau_{i,k}$ is the time cost of passing $SEG_{i,k}$, and s is the physical length of the survey path. In the objective function (Equation (10)), the first term describes the inter-sequence ratio constraints, while the other term states the intra-sequence ratios among segments. By minimizing the objective function, we seek the optimal walking speed estimation that fits the inter- and intra-sequence ratios best. Additionally, we require that the total distance constraint is satisfied (Equation (11)). It is worth noting that our method does not need accurate and explicit input of initial velocities to compute $v_{i,k}$, which is yet required in integration-based methods. The QP above can be solved efficiently using state-of-the-art commercial solvers such as CVXOPT [5].

Given $v_{i,k}$ $(1 \leq i \leq M, 1 \leq k \leq L)$ and the corresponding time duration $\tau_{i,k}$, we can easily calculate the location of each magnetic sample according to Equation (4). To obtain the fingerprint at any desired location $\boldsymbol{l}$ in the path, we take the average magnetic field values from sequences with its assigned physical location most close to $\boldsymbol{l}$.

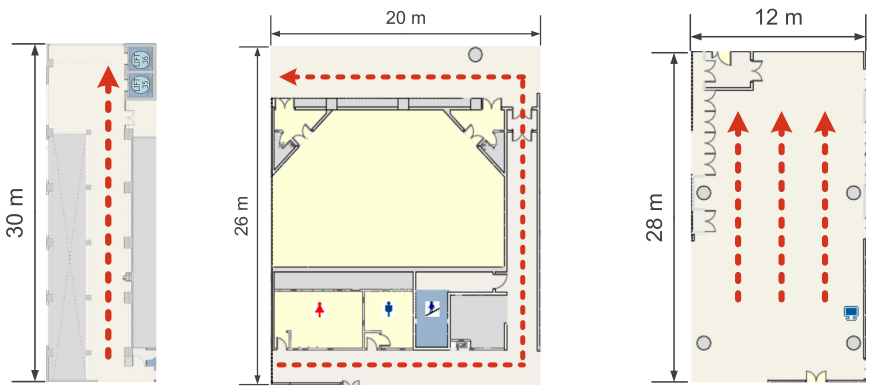

(a) Corridor (b) Mixed area (c) Open area

Fig. 7. The site survey paths in multiple experimental scenarios. The red dotted lines indicate the walking paths and directions in the experiments.

Alternatively, we can replace the path length s in Equation (11) with the unit length 1. Such simplification is reasonable and convenient in practice. Since the pre-planned paths are typically represented as a sequence of coordinates in a floor plan, the normalized distance can help to determine the portions of survey paths that signals lie on. The whole geomagnetic fingerprint database can thus be generated.

6 ILLUSTRATIVE EXPERIMENTAL RESULTS

In this section, we evaluate the accuracy and efficiency of Maficon through experiments. We present the experimental settings and comparison schemes in Section 6.1, followed by illustrative results in Section 6.2. Finally, we demonstrate the localization performance of applying the generated fingerprint database in Section 6.3.

6.1 Experimental Settings

Due to its simplicity and implementability, we have implemented Maficon on the Android platform and tested it on multiple models of COTS mobile phones, including LG Nexus 5, Sony Xperia X2, and Samsung Galaxy S4. Unless otherwise stated, we use Nexus 5 as the default device. These smartphones are all equipped with internal magnetometers and accelerometers. The sampling frequencies are set to be the fastest rate ($\geq$50 Hz).

In our implementation of Maficon, SVR is employed as the default regression model. We select the **radial basis function (RBF)** as its kernel function. The penalty parameter c and kernel width σ in SVR are chosen to maximize the cross-validation performance. We invoke CVXOPT (Python implementation) as the solver for the QP problem [1]. If not otherwise specified, we set the segment length W to be 250 (corresponding to 5 seconds approximately; see Section 3.3).

We have conducted extensive experiments in three typical indoor environments: a corridor (with path length 28.9 m, Figure 7(a)); a larger mixed environment containing corridors, turnings, and open areas (with path length 59.3 m, Figure 7(b)); and a large open space (with path length 18 m, Figure 7(c)). Unless otherwise specified, the corridor site is our default testbed. We invite four volunteers (three males and one female, with different weights and heights ranging from 45 kg to 80 kg and from 1.68 m to 1.8 m, respectively) to participate. Users are required to hold a mobile

Table 3. Survey Path Information in Different Sites

Site	Path Length	#Users	#Devices	Avg. Duration	Duration Range	Avg. Speed	Speed Range*
Corridor	28.9 m	4	3	26.0 s	18.1 s–56.3 s	1.32 m/s	0.69 m/s–2.03 m/s
Mixed area	59.3 m	4	3	48.7 s	41.7 s–57.9 s	1.32 m/s	0.68 m/s–1.88 m/s
Open area	18.0 m × 3	4	3	15.1 s	12.1 s–18.0 s	1.43 m/s	0.81 m/s–2.00 m/s

* The walking speeds are estimated every few seconds from the captured simultaneous video.

phone and walk six times at casual speeds in each environment. We hence collect 360 sequences in total. Detailed information about the survey paths is listed in Table 3.

In this work, we use *walking speed error* and *magnetic fingerprint error* as the performance metrics.

- *Walking speed error*: Walking speed error is defined as the absolute error of the estimated walking speed against the ground-truth speed in each segment. To obtain the ground-truth speeds, we set equispaced labels along the path (1 m between two labels). When the user is walking, we capture a simultaneous video to record the positions and corresponding time. The actual speed is calculated as the ratio of the physical distance between consecutive labels to the time the user passes them.
- *Magnetic fingerprint error*: The magnetic fingerprint error at a certain position is defined as the difference of magnetic field intensity between the generated fingerprint and the ground-truth value. To obtain the ground-truth fingerprints, we stand still and measure magnetic fields at reference positions, which are distributed every 0.2 m along the survey paths. The mean value of magnetic field observations collected at each reference position is treated as the truth value. In addition, the *mean fingerprint error* is calculated by taking the average of fingerprint errors at all reference positions.

We compare Maficon with the following state-of-the-art schemes:

- *Constant speed*: Constant walking speed is a common assumption in the traditional site survey. It assumes that surveyors always walk at constant speeds and thus magnetic field samples are evenly distributed along the path. For each walk, we take the ratio of distance to total time cost as the surveyor's walking speed. The naïve but widely used method can be regarded as the baseline of system performance.
- *Pedometer* (*step counter*) [6]: Pedometer-based approaches infer users' walking speed based on detected steps and stride length. We implement the pedometer by detecting the peaks in the acceleration magnitude sequence [6]. Step length is estimated by following the empirical model $length = K\sqrt[4]{\max(\boldsymbol{A}) - \min(\boldsymbol{A})}$, where $\boldsymbol{A}$ is the magnitude sequence of accelerations within a step and K is a pre-calibrated constant.
- *Supervised learning* [19]: The scheme constructs a regression model associating acceleration features with absolute velocities. The model is obtained through an offline training process. We extract motion features from accelerometer readings collected from several user walks, and the corresponding ground-truth speeds are manually labeled by using the captured simultaneous videos.

6.2 Illustrative Results

We first study the impact of different categories of features used in intra-sequence speed ratio estimation. Specifically, we compare the magnetic field fingerprint errors when using different categories of features, i.e., time-domain features, frequency-domain features, and the combination of them (the feature categories are detailed in Table 2). Figure 8 compares the resulting fingerprint errors in different sites. The vertical error bars indicate the 95% confidence interval.

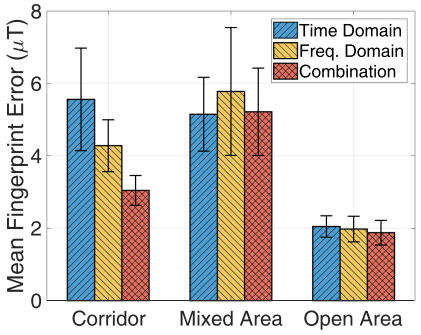

Fig. 8. Magnetic fingerprint error against different categories of features in various sites.

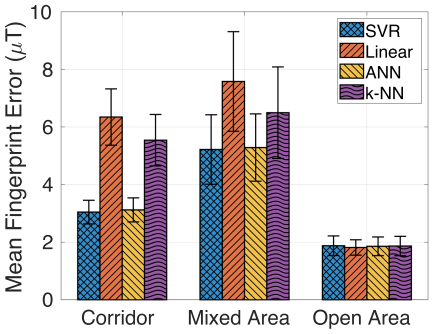

Fig. 9. Magnetic fingerprint error against different regression schemes in various sites.

We can clearly observe that using combined features achieves the lowest fingerprint error and the minimum variance among all scenarios. By contrast, features in neither time domain nor frequency domain alone achieve robust accuracy since they fail to capture users' motion characteristics well. In Maficon, we use the combination of features in the speed ratio model to keep accurate and stable performance.

Figure 9 illustrates the mean fingerprint errors using different regression techniques, i.e., support vector regression (labeled by *SVR*), linear regression (labeled by *Linear*), artificial neural network (labeled by *ANN*), and k-nearest neighbor regression (labeled by *k-NN*). In *ANN*, we construct a three-layer fully connected neural network (with 20, 10, and 2 neurons in each layer, respectively). Though the network does not have a complex structure, it is sufficient to capture the relationship between motion features and speed ratios. In *k-NN*, we seek for the k ($k = 3$) most similar features to the observation and take their average speed ratios as the prediction. We can see that both *SVR* and *ANN* perform accurately and robustly among all the cases. By contrast, linear regression has a larger fingerprint error because the over-simplified model cannot depict the non-linear relationship between features and speed ratio (see Figure 6). Suffering from the scarcity of data, *k-NN* cannot achieve satisfactory performance as well. Considering both accuracy and model tuning difficulties, we choose to use *SVR* for intra-sequence speed ratio estimation.

Figure 10 shows the magnetic fingerprint errors against different segment lengths W, where the vertical error bars indicate 95% confidence interval. We can see that a small W will incur a large error, since the extracted features in a short time window cannot reflect users' walking patterns well. On the other hand, the error gradually increases as W grows. The reason is that a larger segment length decreases the granularity of walking speed estimation, which fails to capture the speed variation. We hence empirically set the segment length $W = 250$ (approximately 5 seconds), which achieves satisfactory accuracy and robustness.

We also study the impact of the number of walks against system performance. In Figure 11, we show the mean fingerprint errors versus the number of input sequences among all users in the corridor. We can see that the fingerprint error decreases as the number of walks increases. The reason is that more sequences provide more knowledge about the speed ratios among both inter- and intra-sequence segments, which effectively reduces the estimation errors and enhances the quality of the regression model. Besides, it is worth noting that the performance gain becomes smaller when the number of walks is greater than five. This is because five sequences have already been sufficient to well-characterize the speed relationships and motion features. Therefore, for balancing accuracy and efficiency, we recommend the number of walks being five in real-world applications.

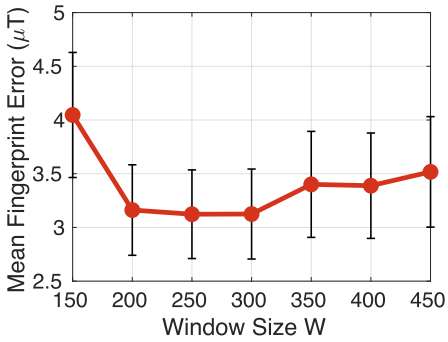

Fig. 10. Magnetic fingerprint errors versus the segment length W.

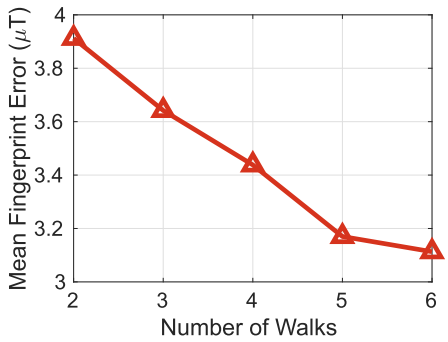

Fig. 11. Magnetic fingerprint errors versus the number of walks.

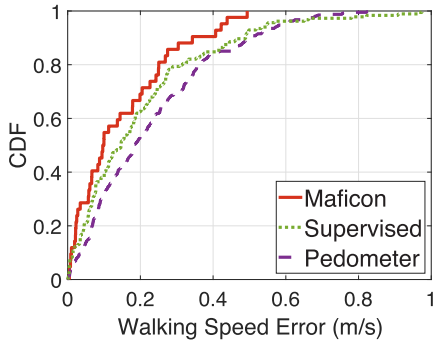

Fig. 12. CDF of walking speed errors in the corridor.

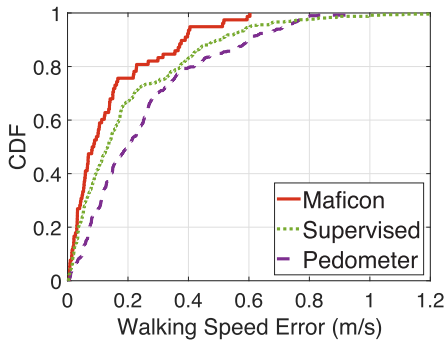

Fig. 13. CDF of walking speed errors in the mixed area.

Since fingerprint generation in Maficon is on the basis of accurate walking speed estimation, we further investigate the accuracy of speed estimation. Figure 12 shows the **cumulative distribution functions (CDFs)** of the walking speed estimation errors in the corridor. We can observe that Maficon achieves the lowest error with the shortest tail. By contrast, the pedometer-based method suffers from its erroneous step length estimation and hence leads to the lowest accuracy. On the other hand, the scheme of supervised learning has a long tail compared with the others. This is mainly because its universal model cannot fit heterogeneous user behaviors perfectly.

Figures 13 and 14 further illustrate the CDFs of walking speed estimation errors in the mixed area and open space, respectively. Similar to the results in the narrow space (Figure 12), Maficon achieves the lowest speed errors and error variance in various types of environments. In the mixed area, the 90th percentile of walking speed error of Maficon is 0.39 m/s, which outperforms the supervised approach and pedometer-based approach by 23.3% (0.50 m/s) and 35.2% (0.60 m/s), respectively. In the open area, Maficon achieves a 90th-percentile speed estimation error of 0.36 m/s, cutting the error of the others by 33.9% (0.54 m/s, supervised approach) and 35.5% (0.55 m/s, pedometer-based approach), respectively.

Figure 15 demonstrates the CDFs of magnetic fingerprint errors in the corridor area compared with the other state-of-the-art schemes. Benefiting from the accurate walking speed estimation, we can see clearly that Maficon outperforms all the other schemes under casual walking. Specifically, Maficon has a mean fingerprint error of 3.12 μT in the corridor, which cuts the error by

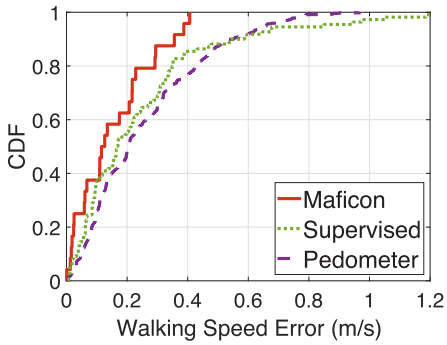

Fig. 14. CDF of walking speed errors in the open area.

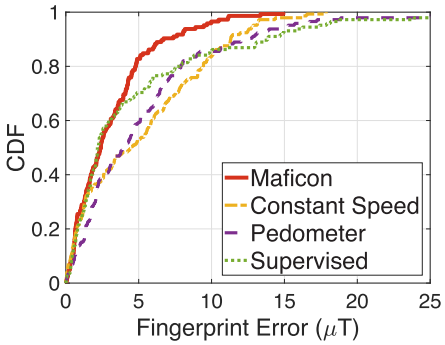

Fig. 15. CDF of magnetic fingerprint errors in the corridor.

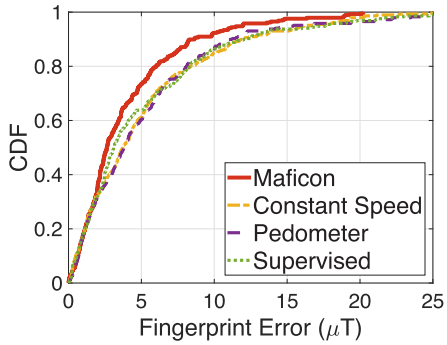

Fig. 16. CDF of magnetic fingerprint errors in the mixed area.

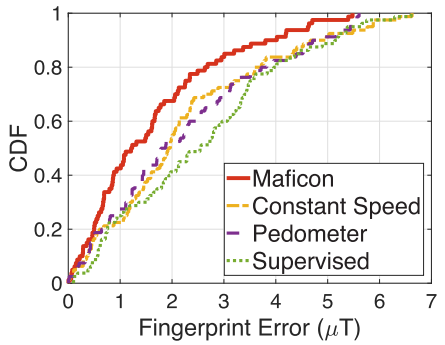

Fig. 17. CDF of magnetic fingerprint errors in the open area.

39.2 % (constant speed), 41.2 % (pedometer), and 36.0 % (supervised learning), respectively. The low fingerprint error guarantees the preciseness of the surveyed fingerprint database.

Figures 16 and 17 further present the CDFs of magnetic fingerprint errors in other scenarios. Maficon has mean fingerprint errors of 3.96 μT in the mixed area and 1.63 μT in the open area. We notice that a longer tail appears in the CDF curve in the mixed area due to high signal variance along the long path (59.3 m). Nevertheless, the tail of Maficon is still shorter than the others. In general, compared with other schemes, Maficon cuts the error by 30.1 % (constant speed), 31.3 % (pedometer), and 31.8 % (supervised learning), respectively. Therefore, Maficon shows its robust performance with a lower fingerprint error against the others regardless of environment types. The results are also consistent with the comparison of walking speed estimation errors in Figures 13 and 14.

To illustrate the adaptivity and robustness of Maficon upon heterogeneous users and devices, we further evaluate fingerprint errors under different users or devices. The upper figure in Figure 18 depicts the fingerprint accuracy of different surveyors using the same device (Nexus 5), while the lower one plots the fingerprint errors when the same surveyor uses different devices. The error bars indicate 95 % confidence interval. The mean errors range from 3.04 μT to 4.21 μT among different users, and ranges from 2.48 μT to 3.04 μT among different devices. We can see that, in both cases, our algorithm presents stably competitive performances against heterogeneity, which validates the adaptivity and robustness of Maficon.

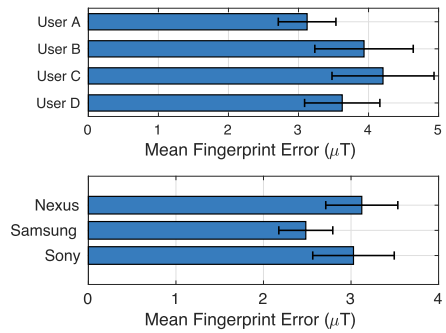

Fig. 18. Fingerprint errors among different users (upper) and devices (lower) in the corridor.

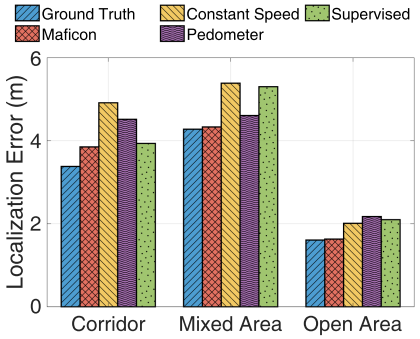

Fig. 19. Localization errors using different fingerprint databases in multiple sites.

6.3 Localization Results

A major purpose of Maficon is to collect fingerprints with accurate location labels for localization. We further conduct experiments to evaluate localization performance on the constructed fingerprint databases. In particular, we implement a classical magnetic field-based localization scheme *Magicol* [22], which employs DTW to seek the most similar magnetic sequences and applies a particle filter to fuse motion information. The experimental venues are the same ones as the previous experiments shown in Figure 7.

We generate multiple magnetic field fingerprint databases using the comparison schemes introduced in Section 6.1. In addition, we conduct a manual site survey to obtain a database as the ground truth. The magnetic field signals are collected by standing still at positions every 0.2 m along each path. Although such point-based manual collection is time-consuming and is not usually applied in practice, it produces an accurate database and can thus be regarded as a good reference for evaluation.

Figure 19 demonstrates the localization errors under the fingerprint databases generated by different methods. We can observe that Maficon achieves a lower error than the other comparison schemes among all scenarios. In detail, Maficon cuts the mean localization error by 21.8% in the corridor, 19.7% in the mixed area, and 18.9% in the open area compared with the system using the database generated under constant speed assumption. In addition, compared with the other approaches, Maficon has a closer performance to the ground-truth database (the localization errors are slightly larger by 12.2%, 2.5%, and 1.4% in the corridor, mixed area, and open area, respectively). We conclude that, among all the competitors, the localization performance of Maficon is the most stable and closest to the one with the ground-truth databases.

7 RELATED WORKS

Fingerprint-based localization has been extensively studied and applied in recent Wi-Fi [11, 13] and geomagnetic localization [14, 22, 25, 31]. LocateMe maps the target locations to the landmarks by observing similar patterns of signal change [25]. Magicol applies a two-pass bidirectional particle filter to fuse magnetic field with traditional Wi-Fi signals [22]. Works in [33] and [27] also apply particle filter techniques to integrate magnetic field with motion information. Mapel employs **conditional random field (CRF)** to infer the target location and adaptively learns a step length model on the fly [31]. All these works discuss how to localize *given* fingerprints and yet have not considered how to construct fingerprints efficiently and accurately. Our work proposes

an accurate and efficient scheme for fingerprint construction, which can be integrated into any existing localization system for fingerprint collection.

To construct fingerprint databases to enable localization, traditional methods collect signals at a large number of pre-defined positions (so-called **reference positions (RPs)**) [12]. However, due to the high spatial variance of magnetic fields, site survey for magnetic fields usually requires denser RPs than RF-based systems (e.g., Wi-Fi), which makes such methods more time-consuming and labor-intensive. Although some works propose to interpolate magnetic fields given a set of sparsely collected samples to reduce efforts [22, 31], the accuracy of the generated fingerprints is still limited. In Maficon, we study an efficient survey enhancement approach for walking-based site surveys, which is orthogonal to the RP-based signal collection.

In modern magnetic site surveys, signals are usually collected while surveyors are walking due to the high sampling rates of COTS smartphones. Though this can effectively speed up the survey process, how to accurately map surveyed signals to physical locations has not been well studied. Most systems assume that the fields are fingerprinted with constant walking speed [7, 30, 33]. This is inconvenient and error-prone. To overcome the requirement by non-constant speed, the pedometer has been proposed in the literature. A pedometer is also known as a step counter, which detects the "steps" of pedestrians based on inertial sensing data such as accelerations and angular velocities. The walking distance can then be estimated by learning user step strides. The work in [37] presents an offline training model to personalize step strides. Brajdic and Harle develop a step counter by clustering the features in time and frequency domains [6]. The work in [32] assumes that different people share similar frequency coefficients of steps and proposes a step length model based on step frequency and user physical profile to estimate stride length. The above work requires a costly offline pre-training process for personalization. Maficon, by contrast, does not depend on any user or step model and requires no explicit calibration or offline training based on manually labeled data. It correlates magnetic fields and user motions by self-training to estimate accurate walking speed.

There have also been many works that explore walking speed estimation without using pedometers. Some works evaluate walking speed based on certain pre-defined human gait models [10, 26]. They usually attach wearable inertial sensors to particular parts of human bodies, such as legs or wrists, which is not convenient, cost-effective, or practical for site surveys. The direct integration method on accelerometer readings has been studied in [2]. However, it requires the knowledge of initial velocity, which is not easy or practical to know in reality [34]. Maficon advances from these works by modeling walking speed estimation as an optimization problem and yields estimations by correlating geomagnetic field signal patterns and accelerometer readings, which is more efficient and practical to deploy. Besides, recent works utilize machine learning for speed estimation. Park et al. study the correlation between motion features and walking speeds [19]. The works in [21] and [24] predict velocities with ANN and **convolutional neural network (CNN)**, respectively. Compared with them, Maficon does not require any manually labeled training data because it is self-trained by leveraging the aligned segments to achieve automatic and personalized calibration.

8 DISCUSSION

We discuss some deployment topics and further potential applications related to Maficon in this section.

Applicability to other signals: Though we discuss in this article the site survey for magnetic fields, Maficon can also be directly applied in path-based collection of other fingerprint signals, e.g., Wi-Fi, **Bluetooth Low Energy (BLE)**, visible lights, etc. On the other hand, Maficon uses magnetic fields to correlate different sequences because of its high sampling frequency (usually tens to hundreds

of samples per second). Lots of existing works have studied the feasibility and effectiveness of using multimodal signals to improve localization performance [8, 18]. Fusing with other location-dependent signals is also a promising direction to enhance the robustness against environmental changes.

Fingerprint collection via implicit crowdsourcing: Since site surveys generally require lots of time and labor resources, it is not cost-efficient to be deployed in large-scale environments. To address this, many works explore implicit crowdsourcing to automatically collect fingerprints, where naïve users collect signals via carried smartphones and their trajectories are inferred offline to obtain signal locations [20, 28]. Maficon is able to integrate into the crowdsourcing schemes for providing better walking speed estimation. By recognizing the common walking paths of different users, Maficon can accurately estimate the speed dynamics of users and hence signal locations.

Application of walking speed estimation: Speed estimation is the core in Maficon. We can also extend the application scenarios of Maficon to real-time speed estimation, such as pathway traffic capacity analysis, walking/running speed estimation in healthcare, trolley speed control in factories, and so forth. We first determine the common walking sub-paths between the target user and previous paths. This can be implemented by adopting the Smith-Waterman algorithm [30]. Given a set of matched sub-paths, Maficon can thus be applied to estimate their movement speeds.

9 CONCLUSION

Previous geomagnetic fingerprinting approaches require constant walking speeds of surveyors or offline calibration using pedometers and user mobility models. To overcome that, we propose Maficon, a novel pedometer-free approach leveraging magnetic fields and accelerometer readings to accurately and efficiently construct a geomagnetism fingerprint database without any manual labeling or training. Maficon greatly simplifies site survey by reducing it to a casual walking process, where a surveyor walks at arbitrary random speeds along pre-defined paths several times. By analyzing the inter- and intra-sequence speed ratios based on magnetic and acceleration patterns sampled from different walks of a path, Maficon adopts self-learning and optimization techniques to accurately estimate walking speed and thus constructs fingerprint databases.

Compared with prior approaches, Maficon requires neither assumptions on user behaviors nor meticulously tuned pedometers. It is computationally efficient and widely deployable to different users, devices, and environments. We have implemented Maficon and conducted extensive experiments at different venues. The experimental studies show that Maficon significantly reduces the walking speed estimation error (by more than 20%) and hence the fingerprint error (by 35% in general) as compared with traditional and state-of-the-art schemes.

REFERENCES

[1] Martin Andersen, Joachim Dahl, and Lieven Vandenberghe. 2005. CVXOPT: A Python Package for Convex Optimization. UCLA.

[2] Stéphane Beauregard and Harald Haas. 2006. Pedestrian dead reckoning: A basis for personal positioning. In *Proceedings of the 3rd Workshop on Positioning, Navigation and Communication*. Shaker, Hannover, Germany, 27–35.

[3] Donald J. Bemdt and James Clifford. 1994. Using dynamic time warping to find patterns in time series. In *Proceedings of 1994 Workshop on Knowledge Discovery in Databases*, Vol. 10. AAAI, Seattle, WA, 359–370.

[4] Christopher Bishop. 2006. *Pattern Recognition and Machine Learning*. Springer, New York, NY.

[5] Stephen P. Boyd and Lieven Vandenberghe. 2004. *Convex Optimization*. Cambridge University Press, Cambridge, UK.

[6] Agata Brajdic and Robert Harle. 2013. Walk detection and step counting on unconstrained smartphones. In *Proceedings of 2013 ACM International Joint Conference on Pervasive and Ubiquitous Computing*. ACM, 225–234. https://doi.org/10.1145/2493432.2493449

[7] Jaewoo Chung, Matt Donahoe, Chris Schmandt, Ig-Jae Kim, Pedram Razavai, and Micaela Wiseman. 2011. Indoor location sensing using geo-magnetism. In *Proceedings of the 9th International Conference on Mobile Systems, Applications, and Services*. ACM, 141–154. https://doi.org/10.1145/1999995.2000010

[8] W. Du, P. Tong, and M. Li. 2021. UniLoc: A unified mobile localization framework exploiting scheme diversity. *IEEE Transactions on Mobile Computing* 20, 7 (July 2021), 2505–2517. https://doi.org/10.1109/TMC.2020.2979857
[9] Rudolf J. Freund, William J. Wilson, and Donna L. Mohr. 2010. *Statistical Methods* (3rd ed.). Academic Press, Cambridge, MA.
[10] Stefan Gradl, Markus Zrenner, Dominik Schuldhaus, Markus Wirth, Tomek Cegielny, Constantin Zwick, and Bjoern M. Eskofier. 2018. Movement speed estimation based on foot acceleration patterns. In *Proceedings of the 40th Annual International Conference of the IEEE Engineering in Medicine and Biology Society*. IEEE, 3505–3508. https://doi.org/10.1109/EMBC.2018.8513042
[11] Suining He and S.-H. Gary Chan. 2016. Tilejunction: Mitigating signal noise for fingerprint-based indoor localization. *IEEE Transactions on Mobile Computing* 15, 6 (June 2016), 1554–1568. https://doi.org/10.1109/TMC.2015.2463287
[12] Suining He and S.-H. Gary Chan. 2016. Wi-Fi fingerprint-based indoor positioning: Recent advances and comparisons. *IEEE Communications Surveys & Tutorials* 18, 1 (2016), 466–490. https://doi.org/10.1109/COMST.2015.2464084
[13] Suining He, S.-H. Gary Chan, Lei Yu, and Ning Liu. 2015. Calibration-free fusion of step counter and wireless fingerprints for indoor localization. In *Proceedings of 2015 ACM International Joint Conference on Pervasive and Ubiquitous Computing*. ACM, 897–908. https://doi.org/10.1145/2750858.2804254
[14] Suining He and Kang G. Shin. 2017. Geomagnetism for smartphone-based indoor localization: Challenges, advances, and comparisons. *Computing Surveys* 50, 6 (Dec. 2017), 97:1–97:37. https://doi.org/10.1145/3139222
[15] Paulien Hogeweg and Ben Hesper. 1984. The alignment of sets of sequences and the construction of phyletic trees: An integrated method. *Journal of Molecular Evolution* 20, 2 (June 1984), 175–186. https://doi.org/10.1007/BF02257378
[16] Konstantin Klipp, Helge Rosé, Jonas Willaredt, Oliver Sawade, and Ilja Radusch. 2018. Rotation-invariant magnetic features for inertial indoor-localization. In *Proceedings of 2018 International Conference on Indoor Positioning and Indoor Navigation*. IEEE, 1–10. https://doi.org/10.1109/IPIN.2018.8533842
[17] Binghao Li, Thomas Gallagher, Andrew G. Dempster, and Chris Rizos. 2012. How feasible is the use of magnetic field alone for indoor positioning? In *Proceedings of 2012 International Conference on Indoor Positioning and Indoor Navigation*. IEEE, 1–9. https://doi.org/10.1109/IPIN.2012.6418880
[18] Zhenguang Liu, Li Cheng, Anan Liu, Luming Zhang, Xiangnan He, and Roger Zimmermann. 2017. Multiview and multimodal pervasive indoor localization. In *Proceedings of the 25th ACM International Conference on Multimedia*. ACM, 109–117. https://doi.org/10.1145/3123266.3123436
[19] Jun-geun Park, Ami Patel, Dorothy Curtis, Seth Teller, and Jonathan Ledlie. 2012. Online pose classification and walking speed estimation using handheld devices. In *Proceedings of 2012 ACM Conference on Ubiquitous Computing*. ACM, 113–122. https://doi.org/10.1145/2370216.2370235
[20] Anshul Rai, Krishna Kant Chintalapudi, Venkata N. Padmanabhan, and Rijurekha Sen. 2012. Zee: Zero-effort crowdsourcing for indoor localization. In *Proceedings of the 18th Annual International Conference on Mobile Computing and Networking*. ACM, 293–304. https://doi.org/10.1145/2348543.2348580
[21] Aawesh Shrestha and Myounggyu Won. 2018. DeepWalking: Enabling smartphone-based walking speed estimation using deep learning. In *Proceedings of 2018 IEEE Global Communications Conference*. IEEE, 1–6. https://doi.org/10.1109/GLOCOM.2018.8647857
[22] Yuanchao Shu, Cheng Bo, Guobin Shen, Chunshui Zhao, Liqun Li, and Feng Zhao. 2015. Magicol: Indoor localization using pervasive magnetic field and opportunistic WiFi sensing. *IEEE Journal on Selected Areas in Communications* 33, 7 (July 2015), 1443–1457. https://doi.org/10.1109/JSAC.2015.2430274
[23] Yuanchao Shu, Kang G. Shin, Tian He, and Jiming Chen. 2015. Last-mile navigation using smartphones. In *Proceedings of the 21st Annual International Conference on Mobile Computing and Networking*. ACM, 512–524. https://doi.org/10.1145/2789168.2790099
[24] Yoonseon Song, Seungchul Shin, Seunghwan Kim, Doheon Lee, and Kwang H. Lee. 2007. Speed estimation from a tri-axial accelerometer using neural networks. In *Proceedings of 29th Annual International Conference of the IEEE Engineering in Medicine and Biology Society*. IEEE, 3224–3227. https://doi.org/10.1109/IEMBS.2007.4353016
[25] Kalyan Pathapati Subbu, Brandon Gozick, and Ram Dantu. 2013. LocateMe: Magnetic-fields-based indoor localization using smartphones. *ACM Transactions on Intelligent Systems and Technology* 4, 4 (Oct. 2013), 73:1–73:27. https://doi.org/10.1145/2508037.2508054
[26] S. Tanaka, K. Motoi, M. Nogawa, and K. Yamakoshi. 2004. A new portable device for ambulatory monitoring of human posture and walking velocity using miniature accelerometers and gyroscope. In *Proceedings of the 26th Annual International Conference of the IEEE Engineering in Medicine and Biology Society*, Vol. 1. IEEE, 2283–2286. https://doi.org/10.1109/IEMBS.2004.1403663
[27] Guohua Wang, Xinyu Wang, Jing Nie, and Liwei Lin. 2019. Magnetic-based indoor localization using smartphone via a fusion algorithm. *IEEE Sensors Journal* 19, 15 (Aug. 2019), 6477–6485. https://doi.org/10.1109/JSEN.2019.2909195
[28] He Wang, Souvik Sen, Ahmed Elgohary, Moustafa Farid, Moustafa Youssef, and Romit Roy Choudhury. 2012. No need to war-drive: Unsupervised indoor localization. In *Proceedings of the 10th International Conference on Mobile Systems, Applications, and Services*. ACM, 197–210. https://doi.org/10.1145/2307636.2307655

[29] Lusheng Wang and Tao Jiang. 1994. On the complexity of multiple sequence alignment. *Journal of Computational Biology* 1 (Jan. 1994), 337–348. https://doi.org/10.1089/cmb.1994.1.337

[30] Hang Wu, Suining He, and S.-H. Gary Chan. 2017. Efficient sequence matching and path construction for geomagnetic indoor localization. In *Proceedings of 2017 International Conference on Embedded Wireless Systems and Networks*. ACM, 156–167.

[31] Hang Wu, Suining He, and S.-H. Gary Chan. 2017. A graphical model approach for efficient geomagnetism-pedometer indoor localization. In *Proceedings of IEEE 14th International Conference on Mobile Ad Hoc and Sensor Systems*. IEEE, 371–379. https://doi.org/10.1109/MASS.2017.11

[32] Zhuoling Xiao, Hongkai Wen, Andrew Markham, and Niki Trigoni. 2015. Indoor tracking using undirected graphical models. *IEEE Transactions on Mobile Computing* 14, 11 (Nov. 2015), 2286–2301. https://doi.org/10.1109/TMC.2015.2398431

[33] Hongwei Xie, Tao Gu, Xianping Tao, Haibo Ye, and Jian Lv. 2014. MaLoc: A practical magnetic fingerprinting approach to indoor localization using smartphones. In *Proceedings of 2014 ACM International Joint Conference on Pervasive and Ubiquitous Computing*. ACM, 243–253. https://doi.org/10.1145/2632048.2632057

[34] Sangki Yun, Yi-Chao Chen, and Lili Qiu. 2015. Turning a mobile device into a mouse in the air. In *Proceedings of the 13th Annual International Conference on Mobile Systems, Applications, and Services*. ACM, 15–29. https://doi.org/10.1145/2742647.2742662

[35] Jiaping Zhao and Laurent Itti. 2018. shapeDTW: Shape dynamic time warping. *Pattern Recognition* 74 (Feb. 2018), 171–184. https://doi.org/10.1016/j.patcog.2017.09.020

[36] Pengfei Zhou, Mo Li, and Guobin Shen. 2014. Use it free: Instantly knowing your phone attitude. In *Proceedings of the 20th Annual International Conference on Mobile Computing and Networking*. ACM, 605–616. https://doi.org/10.1145/2639108.2639110

[37] Wiebren Zijlstra. 2004. Assessment of spatio-temporal parameters during Unconstrained Walking. *European Journal of Applied Physiology* 92, 1 (June 2004), 39–44. https://doi.org/10.1007/s00421-004-1041-5

Received December 2020; revised April 2021; accepted June 2021